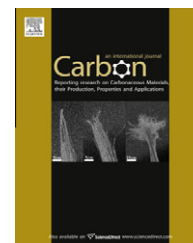


available at [www.sciencedirect.com](http://www.sciencedirect.com)journal homepage: [www.elsevier.com/locate/carbon](http://www.elsevier.com/locate/carbon)

# Electrical double layer capacitors with activated sucrose-derived carbon electrodes

Lu Wei <sup>a,b</sup>, G. Yushin <sup>a,\*</sup>

<sup>a</sup> School of Materials Science and Engineering, Georgia Institute of Technology, Atlanta, GA 30332, USA

<sup>b</sup> School of Materials Science and Engineering, Northwestern Polytechnical University, Xi'an, Shaanxi 710072, PR China

## ARTICLE INFO

### Article history:

Received 28 January 2011

Accepted 2 July 2011

Available online 8 July 2011

## ABSTRACT

Electrical double layer capacitors (EDLCs) with activated sucrose-derived carbons (ASCs) as electrodes are reported. The carbons were prepared by the pyrolysis of sucrose followed by the activation with CO<sub>2</sub> gas for 1–5 h at 900 °C to tune the pore size distribution and the specific surface area (SSA). The porosity of the ASCs has been characterized using N<sub>2</sub> and CO<sub>2</sub> adsorption measurements. The activation increased the SSA from ~200 to 3000 m<sup>2</sup> g<sup>−1</sup> and produced pores mostly in the 0.4–2 nm range. The pyrolysis of sucrose without CO<sub>2</sub> activation produces a carbon with specific capacitance as low as 4 F g<sup>−1</sup>, whereas selected ASCs exhibit specific capacitance in excess of 160 F g<sup>−1</sup> and excellent frequency response in a two-electrode EDLC cell with 1 M H<sub>2</sub>SO<sub>4</sub> electrolyte. The activation time of 4 h resulted in the most promising electrochemical performance. Excellent ASC stability was confirmed by extensive electrochemical characterization after 10,000 charge–discharge cycles.

© 2011 Elsevier Ltd. All rights reserved.

## 1. Introduction

Electrical double layer capacitors (EDLCs), also called electrochemical capacitors, are rechargeable electrical energy storage devices that store more power in a small volume than batteries, but offer lower energy storage capabilities. In contrast to batteries, EDLCs may operate efficiently in a large temperature window, have very long cycle life up to a million (in organic electrolyte), and could be charged in less than 1 min. Their unique characteristics allow them to complement batteries in applications where high power and low weight are essential, including hybrid electrical vehicles, electric motors, peak power and power quality applications [1,2]. The charge in EDLC is stored in a double-layer at the electrode–electrolyte interface. Porous carbons with their relatively low price, high electrical conductivity and high specific surface area (SSA) are used in commercial EDLCs. Carbon nanotubes (CNTs) and carbon nanoparticles with large external surface area commonly offer high rate capability but low

capacitance per unit mass and volume [3–5]. Novel synthesis routes led to the development of high capacitance microporous carbons, using carbide precursors [6–11], inorganic templates [12–16], and a combination of these two approaches [17,18]. Yet, commercial EDLCs still employ activated carbons (ACs) due to their large production volumes and low cost. Recent advancements in ACs [19–22] show that a classical porous carbon synthesis route by pyrolysis of organic compounds followed by activation may remain a viable commercial solution. Petroleum coke and coal used to be the most common materials for AC productions, but the growing global energy demand and an increased awareness of the environmental impacts of fossil fuel combustion led to the AC productions from natural materials, such as nut shells, sugar, corn grain, fibers, sugar cane bagasse, cotton, wood and others [23–30]. In the view of the authors, sugars (and sucrose, in particular) are particularly attractive AC precursors due to their uniform structure (and thus uniform and reproducible properties of the produced ACs, critically important property

\* Corresponding author. Fax: +1 404 8949140.

E-mail address: [yushin@gatech.edu](mailto:yushin@gatech.edu) (G. Yushin).

0008-6223/\$ - see front matter © 2011 Elsevier Ltd. All rights reserved.

doi:10.1016/j.carbon.2011.07.003

for EDLC manufacturers), very low price (within \$0.06–0.15 per kg during the last two decades, according to the United States Department of Agriculture (USDA)), local availability and high chemical purity.

The electrochemical performance of EDLC carbon electrodes is influenced by the electrolyte and various structural parameters of porous carbon, including the microstructure and surface chemistry of carbon [29,21,31], the size of carbon particles [3], SSA [3,7,8,29], pore size [7,8,29] and pore tortuosity [14,17], among a few. The pores smaller than the ion size or highly tortuous pores with bottle-necks may prevent the access of the electrolyte ions to the AC surface and result in a low capacitance and slow frequency response. The pore size and the SSA of the carbonized precursor can be increased by using physical and chemical activation methods. While chemical activation may lead to higher SSA and more uniform pores, it introduces metal ions into the AC, which are challenging and expensive to remove with post-processing. Compared with chemical activation, physical activation using CO<sub>2</sub> or water vapors is simpler and environmentally friendlier process, which has lower cost and does not introduce impurities.

The systematic studies of sucrose-derived carbon's activation and electrochemical evaluation in EDLC have been quite limited. In fact, we have found only one refereed publication, which reported the EDLC performance of activated sugar-derived carbon [32]. The authors prepared their AC by chemical (KOH) activation of sugar and reported the very modest specific capacitance of only ~40 F g<sup>-1</sup>. If improved synthesis conditions would allow the fabrication of better performing AC, the low cost and environment friendly sugar-derived carbon might be considered for the new generation of commercial EDLCs. In this paper, we aimed to study how the porosity in sucrose-derived carbon would change upon simple physical activation and how the change in porosity would affect their electrochemical performance in an aqueous electrolyte.

## 2. Experimental

### 2.1. Activated carbon preparation

Sucrose, DI water and sulfuric acid (H<sub>2</sub>SO<sub>4</sub>) were mixed with mass fraction of 1:0.5:0.1 to form aqueous sucrose/catalyst solution. The solution was pre-heat-treated in a tube furnace under Ar gas (99.9%, Air Gas, USA) flow at 70 °C for 2 h, and then it was heated to 700 °C at a heating rate of 10 °C min<sup>-1</sup> and carbonized for 2 h. After carbonization, the solid carbon samples were cooled down to room temperature under an Ar flow and grinded using a QM-3SP04 planetary ball mill (Across International, USA) at a speed of 400 rpm for 3 h to produce carbon powder. The carbon yield reaches 35.4%, which is close to the theoretical value (42.1%). The powders were subsequently heated to 900 °C under an Ar flow and activated using a pure CO<sub>2</sub> gas (99.9%, Air Gas, USA) flowing at a rate of 50 ml min<sup>-1</sup> for 1 to 5 h. The samples were then cooled under an Ar flow in order to minimize the possible formation of surface groups at elevated temperatures. These carbon samples are tagged as ASC-0 h, ASC-1 h, ASC-2 h, ASC-3 h, ASC-4 h and ASC-5 h with reference to different activation

time. With the increasing of activation time, the mass of carbon sample decreases gradually. After activation, ASC-1 h, ASC-2 h, ASC-3 h, ASC-4 h and ASC-5 h retain 80.8%, 72.1%, 58.5%, 54.8% and 46.2% of the masses before activation, respectively.

### 2.2. Carbon characterization

The carbons were characterized by N<sub>2</sub> adsorption/desorption measurements at -196 °C and CO<sub>2</sub> adsorption at 0 °C using a TriStar II 3020 surface area and porosity analyzer (Micromeritics Instrument Corporation, USA). Before the sorption analyses, the carbon samples were degassed at 300 °C using the VacPrep 061 Degasser (Micromeritics Instrument Corporation, USA) to remove moisture and other adsorbed contaminants. The SSAs ( $S_{\text{BET}}$ ) were calculated from N<sub>2</sub> adsorption isotherms using the Brunauer–Emmett–Teller (BET) equation. Porosity distributions were calculated by the density functional theory (DFT) methods for N<sub>2</sub> and CO<sub>2</sub> adsorption in carbon slit pores. The particle size of carbons was analyzed by using a Hitachi 3500H (Hitachi, Japan) scanning electron microscope (SEM).

### 2.3. Electrochemical measurements

Electrodes were made by mixing 92 wt.% AC and 8 wt.% polytetrafluoroethylene (PTFE) in ethanol to form slurry. The slurry was stirred uniformly and at the same time heated on a hot plate to evaporate most of the ethanol and form a plasticine-like material. The produced AC-PTFE composite was then rolled to ~250 μm thick carbon sheet electrode. The electrode was placed into a vacuum oven (100 °C) overnight to remove the moisture and residual hydrocarbons, and then was cut into the size of 1 cm × 1 cm for EDLC electrodes. Sandwich-type electrochemical cells were set up in a glass beaker with two symmetrical carbon electrodes separated by two 25 μm GORE™ PTFE separators. Gold foil (Alfa Aesar, USA) was attached to each electrode and served as current collectors. 1 M H<sub>2</sub>SO<sub>4</sub> was used as electrolyte.

Cyclic voltammetry (CV) and electrochemical impedance spectroscopy (EIS) measurements were collected using an IM6ex electrochemical workstation (Zahner-elektrok, Germany). CV was performed in the voltage range -600 to +600 mV at scan rates of 1, 10 and 100 mV s<sup>-1</sup>. The equivalent series resistance (ESR) was measured at 10 kHz alternating current. Galvanostatic charge-discharge cycle tests were measured using an Arbin BT-2000 testing system (Arbin Instruments, USA) in the voltage range 0–600 mV and at current loads of 0.1–20 A g<sup>-1</sup>.

## 3. Results and discussion

### 3.1. SEM of samples

Grinding by a ball mill resulted in the carbon powder with irregular morphology and particle size of ~5–15 μm (Fig. 1). Particles smaller than 1 μm were also present but their total volume was less than 5%, according to the SEM image analysis (Fig. 1). The average particle size ~7 μm is typical for ACs

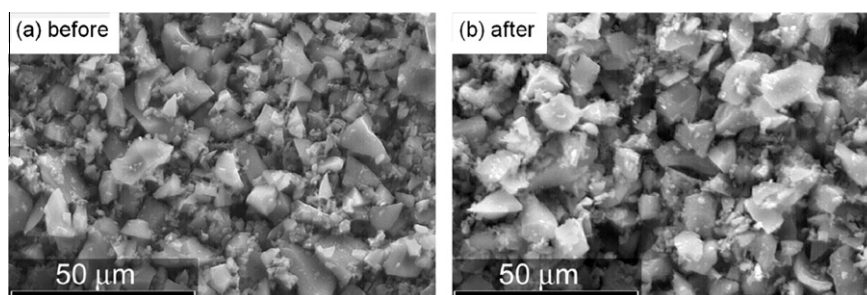


Fig. 1 – SEM micrographs of sucrose-derived carbons: (a) before activation and (b) after activation.

used in commercial EDLCs. The activation with  $\text{CO}_2$  has not changed the particle shape and the particle size distribution to any significant extent (Fig. 1b).

### 3.2. Surface structural properties

To understand the influence of activation conditions on the development of pore structure in carbons prepared from

pyrolysis of sucrose, the ACs were characterized by  $\text{N}_2$  and  $\text{CO}_2$  sorption analyses. The  $\text{N}_2$  sorption isotherms collected at 77 K on sucrose-derived carbons are shown in Fig. 2a. The carbon prepared at 700 °C without any activation (ASC-0 h) adsorbed less than  $60 \text{ cm}^3 \text{ g}^{-1}$  of  $\text{N}_2$  at 0.99 of the relative pressure ( $P/P_0$ ). The employed activation procedure significantly increased the adsorption amount, with all the five AC samples showing  $220\text{--}960 \text{ cm}^3 \text{ g}^{-1}$  adsorption at the highest

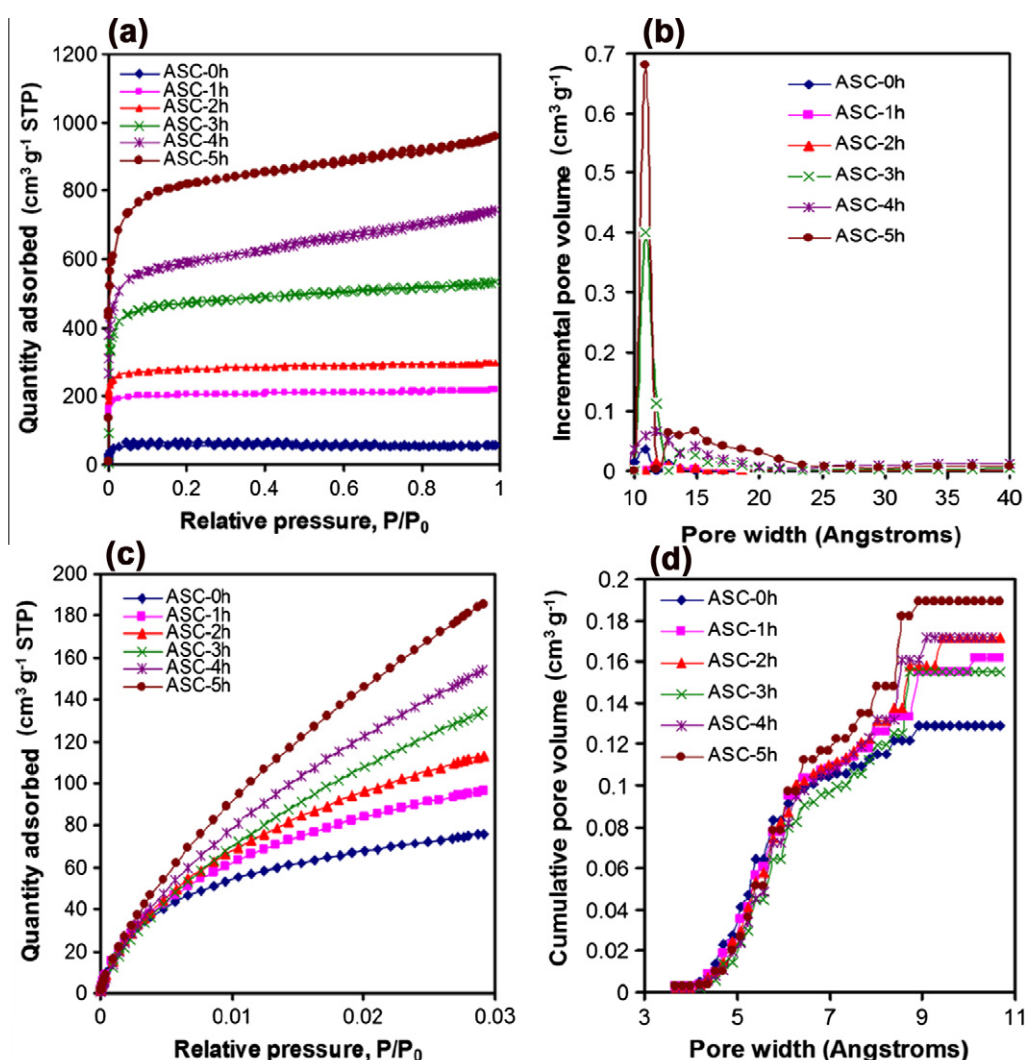


Fig. 2 – Adsorption/desorption isotherms of (a)  $\text{N}_2$  at  $-196^\circ\text{C}$  and (c)  $\text{CO}_2$  at  $0^\circ\text{C}$ , and pore-size distribution derived from (b)  $\text{N}_2$  isotherms at  $-196^\circ\text{C}$  and (d)  $\text{CO}_2$  isotherms at  $0^\circ\text{C}$  for sucrose-derived carbons with different activation time.

relative pressure. The total pore volume (as calculated by measuring the amount of N<sub>2</sub> adsorbed at 0.99 P/P<sub>0</sub>) increases gradually with increasing the activation time (Fig. 2 and Table 1). According to the classification of the International Union of Pure and Applied Chemistry (IUPAC), activated carbons ASC-1 h, ASC-2 h and ASC-3 h exhibit Type I isotherms, which are characteristic of microporous materials. However, the continued slope of the isotherms for ASC-4 h and ASC-5 h above a relative pressure of 0.3 suggests the presence of larger pores in these activated carbons. The hysteresis loops in these samples are very modest, without a clear “knee” visible, suggesting that the effects of capillary condensation are not pronounced and that even the largest pores are smaller than 3–4 nm [33]. The N<sub>2</sub> sorption data are summarized in Table 1. Similarly to the pore volume changes, the SSA of the ACs increase with the CO<sub>2</sub> activation time and ASC-5 h demonstrates SSA as high as 2953 m<sup>2</sup> g<sup>−1</sup> (Table 1). The volume of micropore less than 1 nm was calculated with DFT method from CO<sub>2</sub> adsorption isotherm at 0 °C (Fig. 2c).

The DFT pore-size distribution in Fig. 2b shows that with the increasing of CO<sub>2</sub> activation time, the pore-size of sucrose-derived carbons becomes larger. Yet, the pore size distribution is relatively narrow and mesopores appear only when the activation time exceeds 3 h (Table 1). Interestingly, the volume of pores smaller than 1 nm, is not influenced strongly by the CO<sub>2</sub> activation time (Table 1 and Fig. 2d) and is relatively small even for highly activated samples. These small micropores are believed to be critical for achieving high capacitance values in both organic [7,34] and aqueous [8,34] electrolytes due to the distortion of the solvation shells and closer approach of the ions to the pore walls [35].

### 3.3. Electrochemical measurements

The specific capacitance of sucrose-derived carbon samples has been estimated using CV (Fig. 3). The as-produced carbon sample without activation (ASC-0 h) shows very small specific capacitance (Fig. 3a). The poor electrochemical performance of ASC-0 h cannot be explained only by its low surface area and low pore volume (Table 1) and is likely result from the presence of bottle-neck pores, which were at least partially accessible by N<sub>2</sub> and CO<sub>2</sub> molecules in gas sorption experiments (Fig. 2), but blocked the transport of larger electrolyte ions into the bulk of the carbon particles. The AC samples show no Faradaic peaks in the CVs (note that the Faradaic reactions may still be present), while the non-activated sample has a small peak at 0 V, possibly due to remaining

hydrocarbons or functional groups at the surface. The shortest activation time of 1 h increased the specific capacitance of carbon samples by nearly 40 times (compare Fig. 3a and b), while the surface area and pore volume of this sample increased by less than four times (Table 1). At a scan rate of 1 mV s<sup>−1</sup> the CV curves of all the five AC samples (Fig. 3b–f) show rectangular shape, which is characteristic of an ideal electrochemical double-layer capacitor. The specific capacitance in the range of 130–165 F g<sup>−1</sup> observed for all the synthesized samples is similar to that of the ACs used in commercial EDLC. When the scan rate increases to 100 mV s<sup>−1</sup>, only ASC-4 h and ASC-5 h samples retain rectangular shape, indicating the need of a prolonged (4–5 h) activation to achieve a quick ion transport into the bulk of the particles. This fast ion transport rate makes ASC-4 h and ASC-5 h samples attractive for the applications in high-power EDLCs.

The CO<sub>2</sub> activation significantly lowers the ESR of the carbon samples, as determined by the intersection of the Nyquist plot with the x-axis (real part of the impedance) (Fig. 4a). ASC-4 h and ASC-5 h have the lowest ESR value of ~0.2 Ω cm<sup>2</sup>. The ESR can be approximated as the sum of all the electronic contributions (such as the resistance of the current collectors, carbon electrodes and current collector–electrode interface) and the ionic resistance of the separator. Since activation partially removes the electrode material, this process can likely only decrease the direct current resistance of the carbon electrodes. The current collector and the ionic contributions of the resistance are electrode-independent. Therefore, the obtained results suggest the improvement of the interface resistance upon the carbon activation. Another technologically important parameter is the resistance at the frequency at which nearly all of the charge is stored in a double-layer. This resistance can be obtained by the linear projection of the vertical portion of the Nyquist plot to the real axis. By subtracting the ESR from this resistance one can often estimate the electrolyte resistance in the carbon pores. As expected, the longer activation time evidently lowers the porosity contribution of the total resistance, due to the widening of the pore channel and possibly the narrow portions of the bottle-neck pores (Fig. 2).

The capacitance frequency response of the sucrose-derived carbons with different activation time is presented in Fig. 4b. The specific capacitances are calculated by using the data from the results of EIS [3,14,15,17]. The ASC-4 h sample shows the highest specific capacitance and the best capacitance retention with increasing frequency. The specific capacitance of ASC-4 h drops to half of its maximum value

**Table 1 – Surface structural properties of activated sucrose-derived carbons.**

Sample	S <sub>BET</sub> (m <sup>2</sup> g <sup>−1</sup> )	Pore volume (cm <sup>3</sup> g <sup>−1</sup> )	Micropore (<2 nm) volume (cm <sup>3</sup> g <sup>−1</sup> )	Mesopore (>2 nm) volume (cm <sup>3</sup> g <sup>−1</sup> )	Micropore (<1 nm) volume (cm <sup>3</sup> g <sup>−1</sup> )
ASC-0 h	199	0.07	–	–	–
ASC-1 h	725	0.26	0.25	0.01	0.16
ASC-2 h	992	0.36	0.35	0.01	0.17
ASC-3 h	1687	0.70	0.60	0.10	0.15
ASC-4 h	2102	0.96	0.74	0.22	0.17
ASC-5 h	2953	1.26	1.03	0.23	0.19



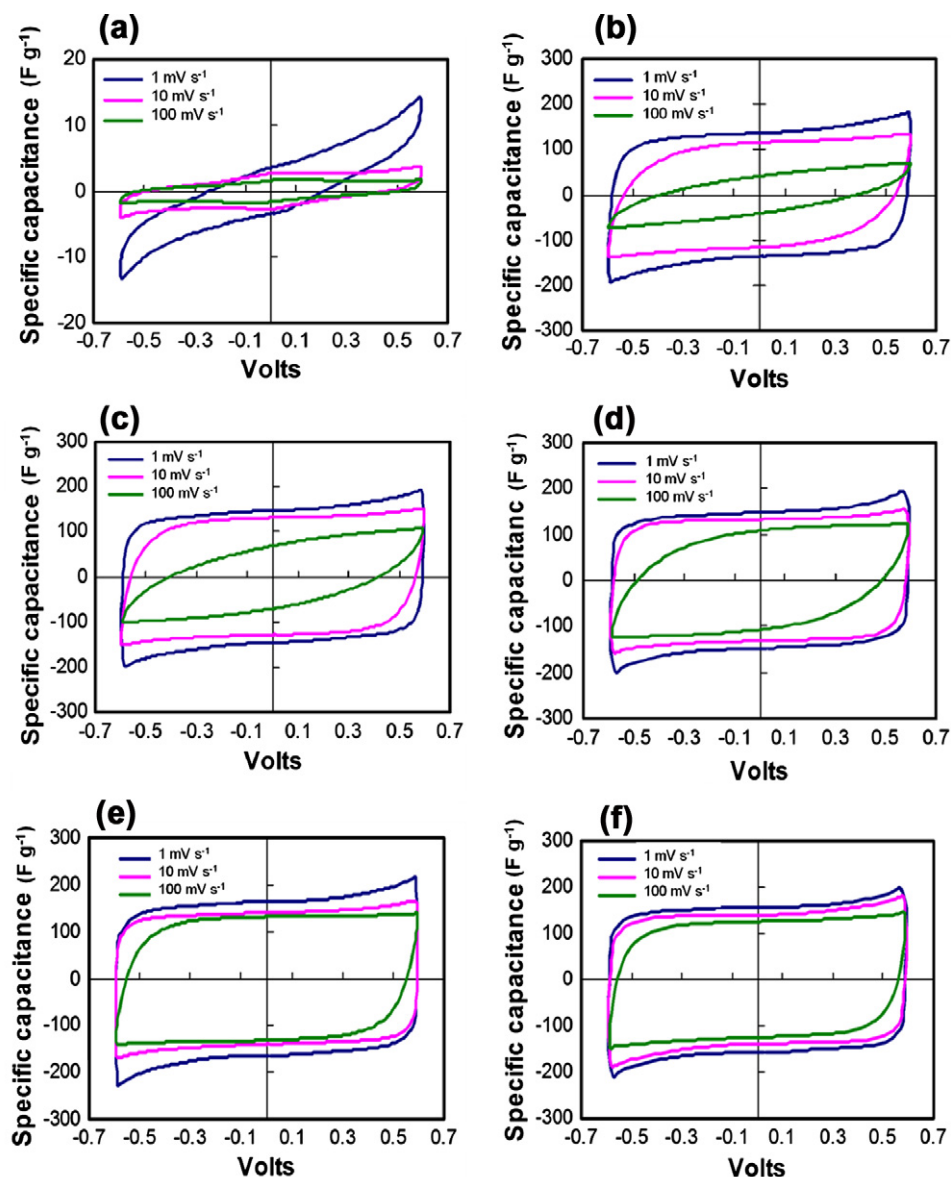


**Fig. 3 – CV curves of sucrose-derived carbons with different activation time (a) ASC-0 h, (b) ASC-1 h, (c) ASC-2 h, (d) ASC-3 h, (e) ASC-4 h and (f) ASC-5 h measured in two-electrode cells.**

( $C/C_{\max} = 0.5$ ) when the frequency increases to 1.42 Hz. While templated carbons with aligned straight pores may demonstrate even higher operating frequency [14], this value is close to the highest measured in commercial ACs (not shown) and is an order of magnitude higher than that observed in carbide-derived carbon [8]. This good frequency response was somewhat pleasantly surprising, considering the relatively large particle size and the small portion of the mesopores in this sample (Fig. 2).

The increase in the highest EDLC operating frequency and in the specific capacitance with increasing the activation time from 1 to 4 h is consistent with CV measurements (Fig. 3) and is likely related to the pore widening (Fig. 2) and increase in SSA (Table 1, Fig. 2). Interestingly, further activation for 1 h (to 5 h total) caused performance deterioration. We hypothesize that excessive activation induces point defects in the

graphene structure, which increase the SSA, but do not provide additional sites for ion adsorption. Due to the defect-solvation shell interactions [31], the over-activated carbons may slow down the ion transport at low rate (compare ASC-4 h and ASC-5 h, Fig. 4b). While the exact mechanisms are still unknown, the capacitance saturation with increasing SSA or activation time is very commonly observed phenomenon in various activated carbons [36].

Fig. 5 shows the influence of activation time on specific capacitance of activated carbon samples at different scan rates. The capacitance values were calculated by using the CV data (Fig. 4). Although ASC-5 h presents the largest total pore volume and specific surface area (Table 1), ASC-4 h shows the highest specific capacitances at all of the scan rates. It is important to note, that the sample activated for a shortest time of 1 h and having the smallest average pore size

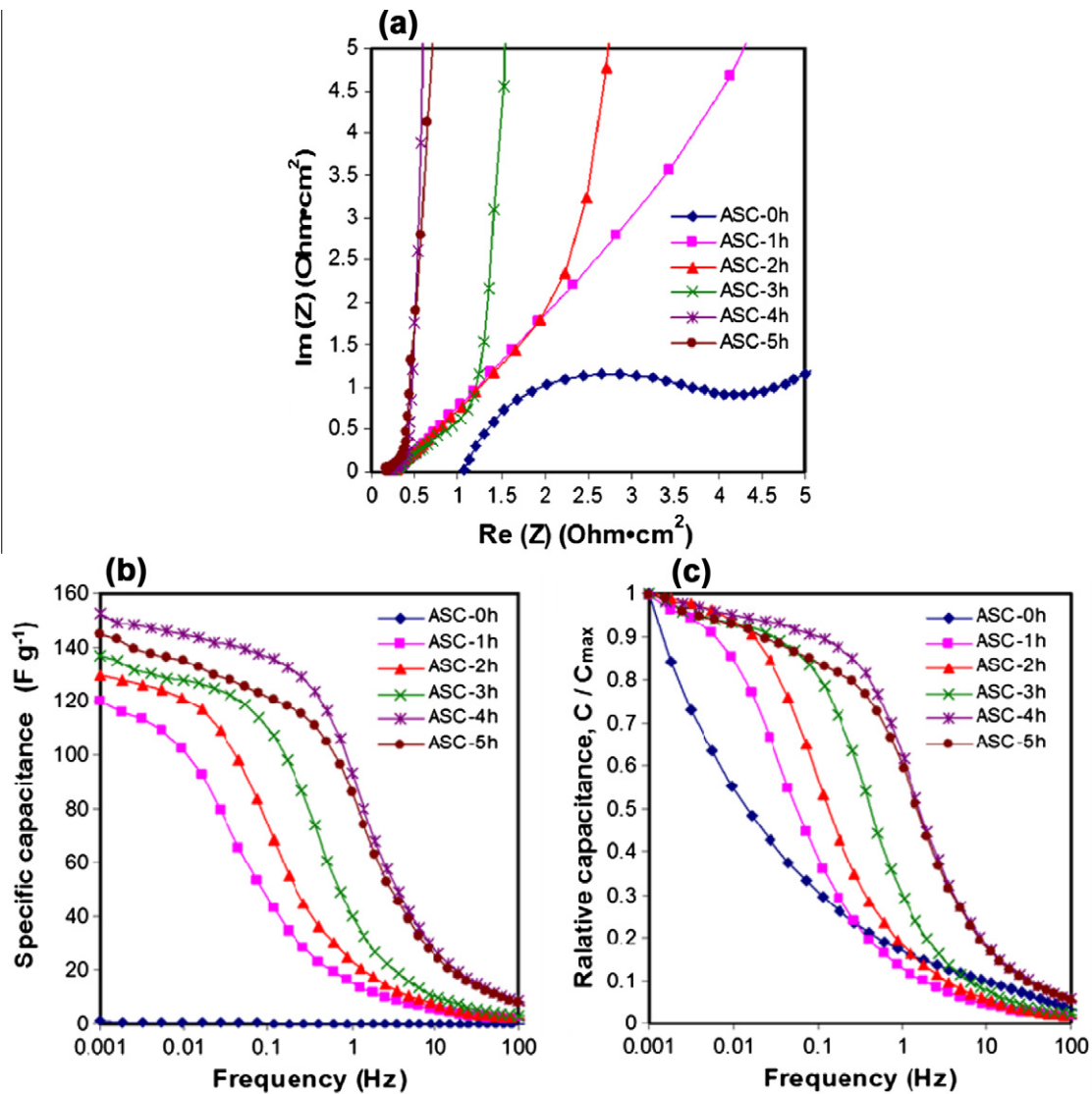


Fig. 4 – (a) Electrochemical impedance spectroscopy and (b) capacitance frequency response of sucrose-derived carbons with different activation time measured in two-electrode cells.

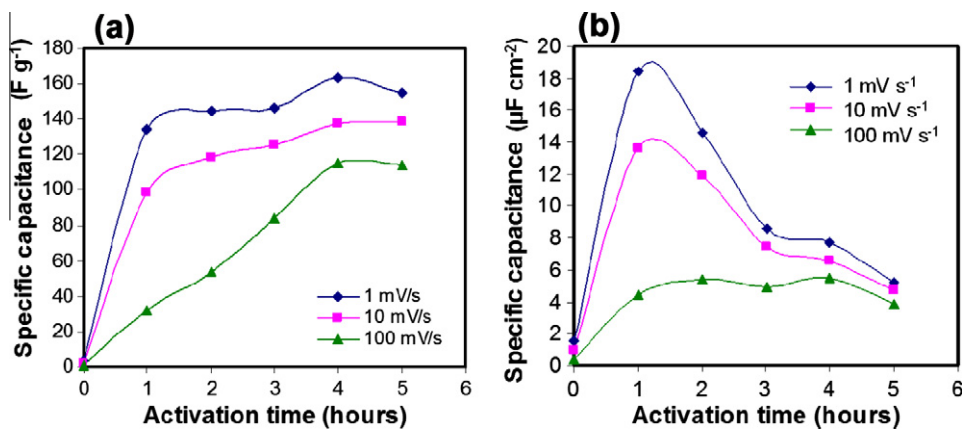


Fig. 5 – Influence of activation time on specific capacitance of activated sucrose-derived carbons at different scan rates.

exhibited the largest capacitance normalized per unit area (Fig. 5b), in accord with previous publications [7,8,29].

The influences of scan rate and current density on specific capacitance of the best sample, ASC-4 h, are shown in Fig. 6.

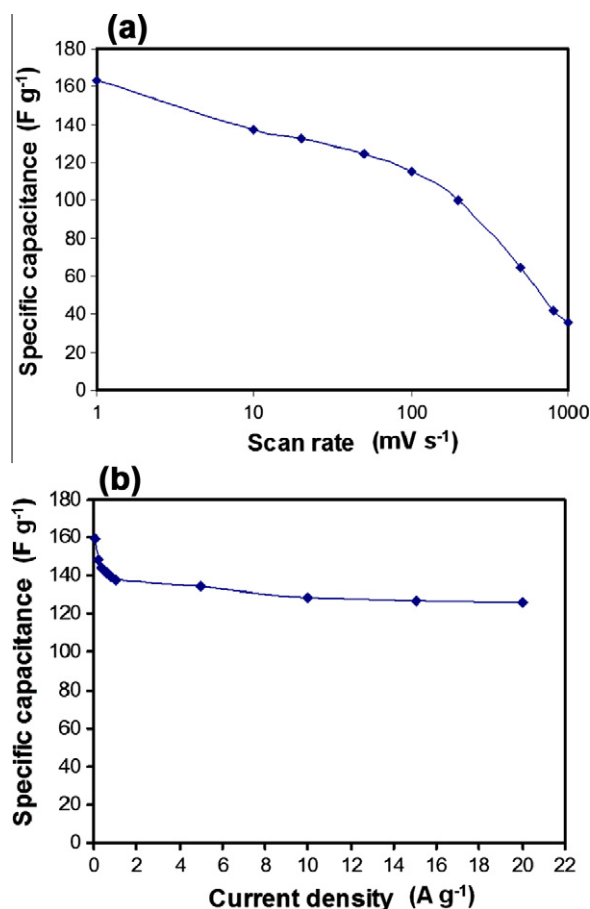


Fig. 6 – Influence of (a) scan rate and (b) current density on specific capacitance of sample ASC-4 h.

The specific capacitances of ASC-4 h at different scan rates in Fig. 6a were obtained from CV (Fig. 4). With scan rate increases from 1 to 1000  $mV s^{-1}$ , the specific capacitances of ASC-4 h gradually decrease from 163 to 35  $F g^{-1}$ . The specific capacitances of ASC-4 h at increasing current loads in Fig. 6b were calculated from charge–discharge cycling curves [15,17]. At current load of 0.1  $A g^{-1}$ , ASC-4 shows the highest capacitance 160  $F g^{-1}$ ; when current load increases to 1  $A g^{-1}$  the capacitance of ASC-4 h decreases to 137  $F g^{-1}$ . However, with the further increase of the current load from 1 to 20  $A g^{-1}$ , the capacitance of ASC-4 h drops slowly. Pores created and widened by the optimum activation procedure act as reservoirs for electrolyte ions and facilitate ion transport through the carbon pore network at fast charge–discharge.

The charge–discharge cycling was carried at current density of 10  $A g^{-1}$ , which presents a current density for a high power application. After 10,000 charge–discharge cycles the ASC-4 h retains rectangular shape of the CV curve at all of the scan rates 1, 10 and 100  $mV s^{-1}$  (Fig. 7), demonstrating the long-term stability of excellent charging and discharging characteristics. Interestingly, after 10,000 charge–discharge cycles ASC-4 h sample exhibited ~4% increasing in specific capacitance (compare Figs. 7 and 4e). The good samples stability was confirmed using EIS tests, where small capacitance increase and no significant changes in the frequency response or ESR were detected (Fig. 8).

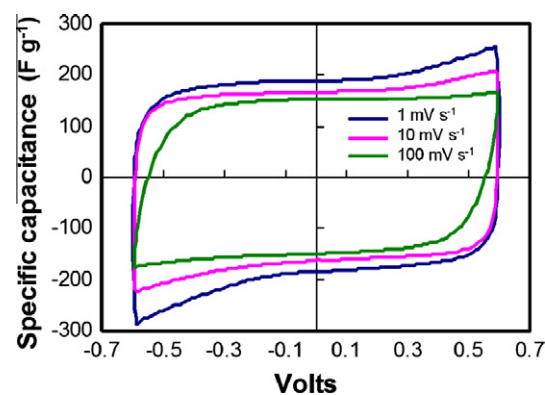


Fig. 7 – CV of ASC-4 h after 10,000 charge–discharge cycles.

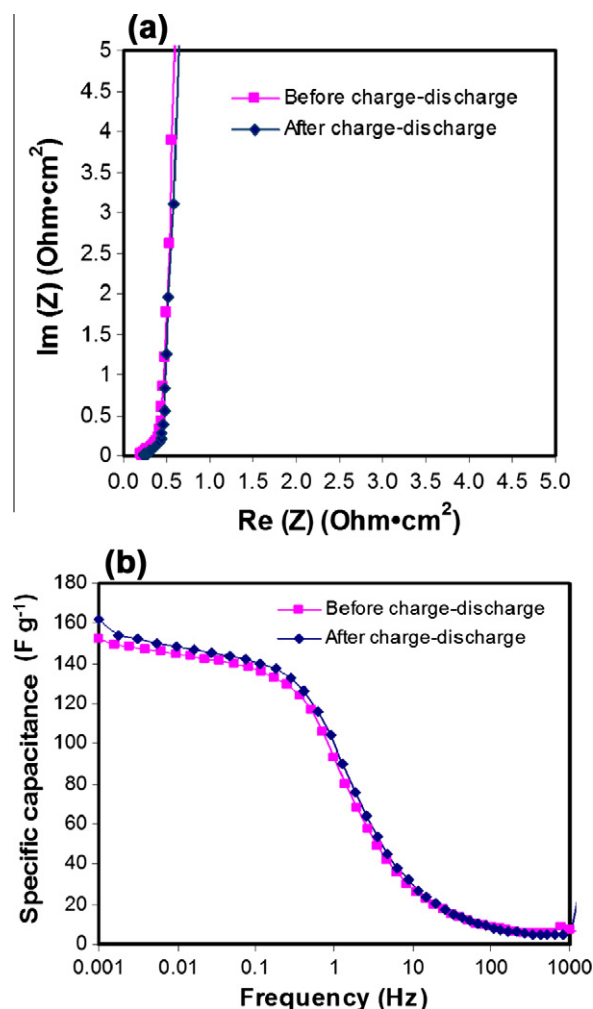


Fig. 8 – (a) Electrochemical impedance spectroscopy and (b) capacitance frequency response of ASC-4 h after 10,000 charge–discharge cycles.

#### 4. Conclusions

The electrochemical performance of activated sucrose-derived carbon electrodes prepared by  $CO_2$  activation at 900 °C was evaluated. Activated carbons with surface areas up to ~3000  $m^2 g^{-1}$  have been produced. The surface area and

volume of mesopores were found to increase with the activation time. While sucrose-derived carbon without activation does not demonstrate a well-developed porosity and good electrochemical performance in EDLC, a simple physical activation with CO<sub>2</sub> allows excellent electrochemical properties to be achieved. The optimum activation time in our experiment was determined to be 4 h. This sample show the ESR as low as 0.2  $\Omega\text{ cm}^2$ , the specific capacitance in excess of 160 F g<sup>-1</sup> and frequency response in excess of 1 Hz in two-electrode EDLC cell containing 1 M H<sub>2</sub>SO<sub>4</sub> electrolyte. After 10,000 charge–discharge cycles at current density of 10 A g<sup>-1</sup>, this sample demonstrated 4% increase in the specific capacitance and no noticeable degradation in the frequency response or ESR. The performed tests suggest that activated sucrose-derived carbons show great promise as a low-cost renewable electrode material for EDLC.

## Acknowledgment

This project was partially supported by a gift from a Semiconductor Research Corporation.

## REFERENCES

- [1] Conway BE. Electrochemical supercapacitors: science fundamentals and technology applications. New York: Kluwer-Plenum; 1999.
- [2] Simon P, Gogotsi Y. Materials for electrochemical capacitors. *Nat Mater* 2008;7(11):845–54.
- [3] Portet C, Yushin G, Gogotsi Y. Effect of carbon particle size on electrochemical performance of EDLC. *J Electrochem Soc* 2008;155(7):A531–6.
- [4] Chen JH, Li WZ, Wang DZ, Yang SX, Wen JG, Ren ZF. Electrochemical characterization of carbon nanotubes as electrode in electrochemical double-layer capacitors. *Carbon* 2002;40(8):1193–7.
- [5] Frackowiak E, Beguin F. Electrochemical storage of energy in carbon nanotubes and nanostructured carbons. *Carbon* 2002;40(10):1775–87.
- [6] Cambaz ZG, Yushin GN, Gogotsi Y, Vyshnyakova KL, Pereselentseva LN. Formation of carbide-derived carbon on beta-silicon carbide whiskers. *J Am Ceram Soc* 2006;89(2):509–14.
- [7] Chmiola J, Yushin G, Gogotsi Y, Portet C, Simon P, Taberna PL. Anomalous increase in carbon capacitance at pore sizes less than 1 nanometer. *Science* 2006;313(5794):1760–3.
- [8] Chmiola J, Yushin G, Dash R, Gogotsi Y. Effect of pore size and surface area of carbide derived carbons on specific capacitance. *J Power Sources* 2006;158(1):765–72.
- [9] Yushin G, Hoffman EN, Barsoum MW, Gogotsi Y, Howell CA, Sandeman SR, et al. Mesoporous carbide-derived carbon with porosity tuned for efficient adsorption of cytokines. *Biomaterials* 2006;27(34):5755–62.
- [10] Leis J, Arulepp M, Kuura A, Latt M, Lust E. Electrical double-layer characteristics of novel carbide-derived carbon materials. *Carbon* 2006;44(11):2122–9.
- [11] Hoffman EN, Yushin G, El-Raghy T, Gogotsi Y, Barsoum MW. Micro and mesoporosity of carbon derived from ternary and binary metal carbides. *Microporous Mesoporous Mater* 2008;112(1–3):526–32.
- [12] Kyotani T, Ma ZX, Tomita A. Template synthesis of novel porous carbons using various types of zeolites. *Carbon* 2003;41(7):1451–9.
- [13] Nishihara H, Itoi H, Kogure T, Hou PX, Touhara H, Okino F, et al. Investigation of the ion storage/transfer behavior in an electrical double-layer capacitor by using ordered microporous carbons as model materials. *Chem Eur J* 2009;15(21):5355–63.
- [14] Kajdos A, Kvit A, Jones F, Jagiello J, Yushin G. Tailoring the pore alignment for rapid ion transport in microporous carbons. *J Am Chem Soc* 2010;132(10):3252–3.
- [15] Portet C, Yang Z, Korenblit Y, Gogotsi Y, Mokaya R, Yushin G. Electrical double-layer capacitance of zeolite-templated carbon in organic electrolyte. *J Electrochem Soc* 2009;156(1):A1–6.
- [16] Ania CO, Khomenko V, Raymundo-Pinero E, Parra JB, Beguin F. The large electrochemical capacitance of microporous doped carbon obtained by using a zeolite template. *Adv Funct Mater* 2007;17(11):1828–36.
- [17] Korenblit Y, Rose M, Kockrick E, Borchardt L, Kvit A, Kaskel S. High-rate electrochemical capacitors based on ordered mesoporous silicon carbide-derived carbon. *ACS Nano* 2010;4(3):1337–44.
- [18] Rose M, Korenblit Y, Kockrick E, Borchardt L, Oschatz M, Kaskel S, et al. Hierarchical micro- and mesoporous carbide-derived carbon as a high-performance electrode material in supercapacitors. *Small* 2011;7(8):1108–17.
- [19] Hulicova-Jurcakova D, Kodama M, Shiraishi S, Hatori H, Zhu ZH, Lu GQ. Nitrogen-enriched nonporous carbon electrodes with extraordinary supercapacitance. *Adv Funct Mater* 2009;19(11):1800–9.
- [20] Hulicova-Jurcakova D, Seredych M, Lu GQ, Bandoz TJ. Combined effect of nitrogen- and oxygen-containing functional groups of microporous activated carbon on its electrochemical performance in supercapacitors. *Adv Funct Mater* 2009;19(3):438–47.
- [21] Barpanda P, Li YL, Cosandey F, Rangan S, Bartynski RA, Amatuucci GG. Fabrication, physical and electrochemical investigation of microporous carbon polyiodide nanocomposites. *J Electrochem Soc* 2009;156(11):A873–85.
- [22] Wei L, Sevilla M, Fuertesc AB, Mokaya R, Yushin G. Hydrothermal carbonisation of abundant renewable natural organic chemicals for high-performance supercapacitor electrodes. *Adv Energy Mater* 2011;1(3):356–61.
- [23] Adib F, Bagreev A, Bandoz TJ. Analysis of the relationship between H<sub>2</sub>S removal capacity and surface properties of unimpregnated activated carbons. *Environ Sci Technol* 2000;34(4):686–92.
- [24] Rufford TE, Hulicova-Jurcakova D, Khosla K, Zhu ZH, Lu GQ. Microstructure and electrochemical double-layer capacitance of carbon electrodes prepared by zinc chloride activation of sugar cane bagasse. *J Power Sources* 2010;195(3):912–8.
- [25] Li QY, Wang HQ, Dai QF, Yang JH, Zhong YL. Novel activated carbons as electrode materials for electrochemical capacitors from a series of starch. *Solid State Ionics* 2008;179(7–8):269–73.
- [26] Balathanigaimani MS, Shim WG, Lee MJ, Kim C, Lee JW, Moon H. Highly porous electrodes from novel corn grains-based activated carbons for electrical double layer capacitors. *Electrochem Commun* 2008;10(6):868–71.
- [27] Wu FC, Tseng RL, Hu CC, Wang CC. Effects of pore structure and electrolyte on the capacitive characteristics of steam- and KOH-activated carbons for supercapacitors. *J Power Sources* 2005;144(1):302–9.
- [28] Subramanian V, Luo C, Stephan AM, Nahm KS, Thomas S, Wei BQ. Supercapacitors from activated carbon derived from banana fibers. *J Phys Chem C* 2007;111(20):7527–31.



- 
- [29] Salitra G, Soffer A, Eliad L, Cohen Y, Aurbach D. Carbon electrodes for double-layer capacitors. I: Relations between ion and pore dimensions. *J Electrochem Soc* 2000;147(7):2486–93.
- [30] Wei L, Yushin G. Electrical double layer capacitors with sucrose derived carbon electrodes in ionic liquid electrolytes. *J Power Sources* 2011;196(8):4072–9.
- [31] Portet C, Yushin G, Gogotsi Y. Electrochemical performance of carbon onions, nanodiamonds, carbon black and multiwalled nanotubes in electrical double layer capacitors. *Carbon* 2007;45(13):2511–8.
- [32] Huang XW, Xie ZW, Qu XG, Wang QW, Qu LY, Xie DM. Properties of electric double-layer capacitors using activated carbon prepared from pyrolytic treatment of sugar as their electrodes. *Chem J Chin U* 2002;23(2):291–3.
- [33] Yang RT. Adsorbents: fundamentals and applications. Hoboken, NJ: John Wiley & Sons; 2003.
- [34] Raymundo-Pinero E, Kierzek K, Machnikowski J, Beguin F. Relationship between the nanoporous texture of activated carbons and their capacitance properties in different electrolytes. *Carbon* 2006;44(12):2498–507.
- [35] Huang JS, Sumpter BG, Meunier V. Theoretical model for nanoporous carbon supercapacitors. *Angew Chem Int Ed* 2008;47(3):520–4.
- [36] Barbieri O, Hahn M, Herzog A, Kotz R. Capacitance limits of high surface area activated carbons for double layer capacitors. *Carbon* 2005;43(6):1303–10.